Switched Control of Cadence During Stationary Cycling Induced by Functional Electrical Stimulation

Matthew J. Bellman, Teng-Hu Cheng, Ryan J. Downey, Chris J. Hass, and Warren E. Dixon

***Abstract*—Functional electrical stimulation (FES) can be used to activate the dysfunctional lower limb muscles of individuals with neurological disorders to produce cycling as a means of rehabilitation. However, previous literature suggests that poor muscle control and nonphysiological muscle fiber recruitment during FES-cycling causes lower efficiency and power output at the cycle crank than able-bodied cycling, thus motivating the investigation of improved control methods for FES-cycling. In this paper, a stimulation pattern is designed based on the kinematic effectiveness of the rider's hip and knee joints to produce a forward torque about the cycle crank. A robust controller is designed for the uncertain, nonlinear cycle-rider system with autonomous, state-dependent switching. Provided sufficient conditions are satisfied, the switched controller yields ultimately bounded tracking of a desired cadence. Experimental results on four able-bodied subjects demonstrate cadence tracking errors of 0.05±1.59 and 5.27±2.14 revolutions per minute during volitional and FES-induced cycling, respectively. To establish feasibility of FES-assisted cycling in subjects with Parkinson's disease, experimental results with one subject demonstrate tracking errors of 0.43±4.06 and 0.17±3.11 revolutions per minute during volitional and FES-induced cycling, respectively.**

***Index Terms*—Functional electrical stimulation (FES), Lyapunov methods, medical control systems, switched control.**

I. Introduction

FUNCTIONAL electrical stimulation (FES) is the application of electrical current across muscle fibers to artificially induce a muscle contraction and achieve a functional outcome (e.g., limb motion). Since the 1980s, FES has been applied to the lower limb muscles of people with upper motor neuron lesions (e.g., following spinal cord injury or stroke) to enable them to pedal a stationary cycle [1], and numerous physiological and psychological benefits have since been demonstrated. Specifically, physiological benefits of FES-cycling such as improved cardiovascular health, increased muscle mass and bone mineral density, decreased spasticity, and improved lower limb function, as well as psychological benefits such as improved self-image, independence, and socialization, have been reported for individuals with spinal cord injury, stroke, cerebral palsy, and multiple sclerosis [2]. To supplement these benefits with enhanced locomotion, mobile FES-cycling devices have been developed [3]–[9] and even commercialized.[1]

Various FES-cycling studies have examined open-loop or proportional-derivative feedback control of the stimulation intensity to achieve a desired cycling cadence [3]–[5], [7], [10]–[12]. Motivated to improve FES-cycling performance, researchers have investigated linear model identification and pole placement methods [8], [13], [14], fuzzy logic control [15], [16], neural network feedforward in addition to proportional-derivative feedback control [17], [18], and higher order sliding mode combined with fuzzy logic control [19]. All of these previous FES-cycling control studies had cadence tracking as a primary control objective, as cadence is one of the most important factors in cycling interventions for rehabilitation [20]. In addition, all of these previous studies used a switched control input that alternated stimulation across different muscle groups according to a predefined stimulation pattern. The stimulation pattern defines the segments of the crank cycle over which each muscle group is stimulated to achieve the desired cycling motion and is: manually determined [1], [3], [7], [8], [11], [21], determined from offline numerical optimization [10], [17], [22]–[24], analytically determined [15], or based on able-bodied electromyography (EMG) measurements [4], [5], [12], [25].

Switching the stimulation control input between multiple muscle groups according to the cycle crank angle makes the overall FES-cycling system a switched control system with autonomous, state-dependent switching [26, Sec. 1.1.3]. In general, during FES-cycling, there exist periods during which one or more muscle groups are active followed by periods during which no muscle groups are active. When muscle groups are actively controlled by stimulation, the system may track the desired trajectory, but when no muscle groups are active, the system becomes uncontrolled. This behavior is complicated by the fact that the dynamics of FES-cycling are

Manuscript received May 18, 2015; revised August 28, 2015; accepted October 15, 2015. Date of publication November 13, 2015; date of current version December 06, 2016. Research for this paper was conducted with Government support under FA9550-11-C-0028 and awarded by the Department of Defense, Air Force Office of Scientific Research, National Defense Science and Engineering Graduate (NDSEG) Fellowship 32 CFR 168a. This work was supported in part by the National Science Foundation under Award 1161260.

M. J. Bellman, T.-H. Cheng, R. J. Downey, and W. E. Dixon are with the Department of Mechanical and Aerospace Engineering, University of Florida, Gainesville FL 32611-6250 USA (e-mail: mattjo@ufl.edu; tenghu@ufl.edu; ryan2318@ufl.edu; wdixon@ufl.edu).

C. J. Hass is with the Department of Applied Physiology and Kinesiology, University of Florida, Gainesville FL 32611-6250 USA (e-mail: cjhass@hhp.ufl.edu).

Color versions of one or more of the figures in this paper are available online at http://ieeexplore.ieee.org.

Digital Object Identifier 10.1109/TNSRE.2015.2500180

[1]http://www.hasomed.de/en/products/rehabike-cycling-with-fes.html; http://www.berkelbike.co.uk/

nonlinear, time-varying, and uncertain, so that the system's state trajectories (e.g., cadence) are unknown *a priori*. None of the aforementioned studies have explored FES-cycling control while considering these properties of the FES-cycling system. Investigating FES-cycling in the light of switched systems theory may yield control strategies that improve FES-cycling performance, thereby increasing the safety and effectiveness of FES-cycling.

In this paper, a nonlinear model of a stationary FES-cycling system is developed that includes parametric uncertainty and an unknown, bounded, time-varying disturbance, similar to the earlier work in [27] but further developed to consider the effects of switching across multiple muscle groups. Extending the preliminary work in [28], a stimulation pattern for the gluteal, quadriceps femoris, and hamstrings muscle groups is designed based on the kinematic effectiveness of the rider's hip and knee joints to produce a forward torque about the cycle crank. A switched sliding mode control input is developed based on this stimulation pattern with the objective that the rider pedal at a desired cadence. A common Lyapunov-like function is used to prove that the cadence tracking error is bounded by an exponentially decaying envelope in regions where muscle groups are activated and by an exponentially increasing envelope in regions where no muscle groups are activated. The overall error system is shown to be ultimately bounded provided sufficient conditions on the control gains, desired trajectory, and stimulation pattern are satisfied. Experimental results on able-bodied subjects demonstrate the switched controller's performance under typical FES-cycling conditions.

Although FES-cycling is typically utilized for individuals with spinal cord injuries, its benefits have been demonstrated for individuals with cerebral palsy, multiple sclerosis, and stroke [2], and FES-cycling may also benefit other populations with movement disorders. For example, Parkinson's disease (PD) is a neurodegenerative disorder that causes both motor (e.g., decline in muscle force production, rigidity, postural instability, and tremor) and nonmotor (e.g., fatigue, anxiety, and depression) symptoms. Bradykinesia (slowness of movement) and muscle weakness are common in persons with PD and can be derived from the reduction in the excitatory drive to the motor cortex and ultimately the muscles. Exercise, especially in the form of assisted (i.e., forced) cycling, is an effective treatment for the motor symptoms of PD [29], [30]. It has been demonstrated that assisted cycling, where the rider pedals with external assistance at a rate greater than the preferred voluntary rate, yields greater improvements in motor and central nervous system function in people with PD when compared to voluntary cycling. Further, it has been suggested that the mechanism for these improvements may be the increased quantity and quality of intrinsic feedback during assisted cycling [29]. It has also been demonstrated that cueing training improves motor performance in people with PD [30]. Therefore, FES-assisted cycling, where FES is applied in addition to the rider's effort to voluntarily pedal at a prescribed cadence, has the potential to improve motor performance in people with PD, as the added FES can enhance muscle force production and provide cueing via the sensation of the stimulation during cycling. Since previous studies have not investigated the use of FES-assisted

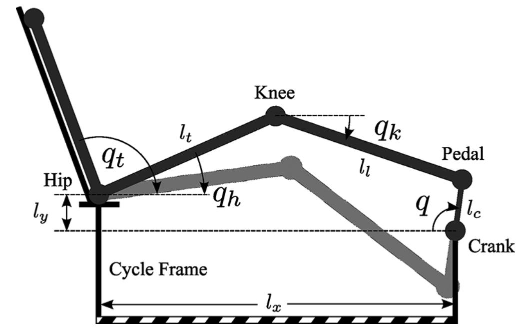

Fig. 1. Model of the cycle-rider system. The joint angles q_t, q_h, q_k, and q denote the trunk, hip, knee, and crank joint angles, respectively, relative to the horizontal. The lengths l_x, l_y, l_t, l_l, and l_c denote the horizontal and vertical seat position, the thigh length, the lumped shank length, and the cycle crank length, respectively.

cycling in people with PD, this paper provides the results of an experiment conducted with one subject with PD to establish feasibility of FES-assisted cycling in this population, and it is demonstrated that FES-assisted cycling has the potential to improve the cycling performance of people with PD.

II. Model

A. Stationary Cycle and Rider Dynamic Model

A two-legged rider pedaling a recumbent stationary cycle can be modeled as a single degree-of-freedom system [31], which can be expressed as

$$M\ddot{q} + V\dot{q} + G = \tau_{\text{crank}} \tag{1}$$

where $q \in \mathcal{Q} \subseteq \mathbb{R}$ denotes the crank angle as defined in Fig. 1; $M,\ V,\ G \in \mathbb{R}$ denote the effects of inertia, centripetal and Coriolis, and gravitational effects, respectively, of the combined rider and cycle about the crank axis; and $\tau_{\text{crank}} \in \mathbb{R}$ denotes the net external torque applied about the crank axis. The recumbent stationary cycle is modeled as having three links (one link is fixed to the ground) representing the cycle frame and seat and three revolute joints representing the cycle crank and the two pedals. The other two rigid links represent the pedal crank arms, which rotate about the crank joint with a constant phase difference of π radians and terminate with a revolute joint representing a pedal. Each of the rider's legs is modeled as a two-link, serial kinematic chain with a revolute joint fixed to the cycle seat (hip joint) and another revolute joint joining the links (knee joint). The ankle joint is assumed to be fixed in the anatomically neutral position in accordance with common clinical cycling practices for safety and stability [32]. The rider's feet are fixed to the cycle pedals, constraining the rider's legs to rotation in the sagittal plane and closing the kinematic chain. The resulting system, depicted in Fig. 1, is reduced to a single degree-of-freedom and therefore can be completely described by the crank angle (or any other single joint angle measured with respect to ground) and the rider's and cycle's link lengths. In Fig. 1, $q_t \in \mathbb{R}$ denotes the rider's trunk angle with respect to ground, and $q_h,\ q_k \in \mathbb{R}$ denote the measurable hip and knee angles, respectively, which are geometric functions of the measurable constant horizontal and vertical distance between the hip and crank joint axes, $l_x,\ l_y \in \mathbb{R}_{\geq 0}$, and the measurable constant thigh, shank, and crank arm lengths, $l_t,\ l_l,\ l_c \in \mathbb{R}_{>0}$, respectively.

In this development, the external torque applied about the crank axis is expressed as

$$\tau_{\text{crank}} = \tau_a + \tau_p + \tau_b + \tau_d \tag{2}$$

where $\tau_a,\ \tau_p,\ \tau_b,\ \tau_d \in \mathbb{R}$ denote the torques applied about the crank axis by active muscle forces, passive viscoelastic tissue forces, viscous crank joint damping, and disturbances (e.g., spasticity or changes in load), respectively. The viscous crank joint damping term τ_b is modeled as $\tau_b \triangleq -c\dot{q}$, where $c \in \mathbb{R}_{>0}$ is the unknown, constant damping coefficient that has a known, constant upper bound $c_b \in \mathbb{R}_{>0}$.

Assumption 1: The biarticular effects of the rectus femoris and hamstring muscles are negligible.

The active torque resulting from stimulation of the gluteal (glute), quadriceps femoris (quad), and hamstrings (ham) muscle groups can be expressed as

$$\tau_a \triangleq \sum_{s\in\mathcal{S}} \sum_{m\in\mathcal{M}} v_m^s \Omega_m^s T_m^s \tag{3}$$

where $v_m^s \in \mathbb{R}$ denotes the subsequently designed stimulation intensity input to each muscle group, $\Omega_m^s \in \mathbb{R}$ denotes the relationship between stimulation intensity and a muscle's resultant torque about the joint it spans, and $T_m^s \in \mathbb{R}$ denotes the Jacobian elements relating a muscle's resultant joint torque to torque about the crank axis. The superscript $s \in \mathcal{S} \triangleq \{R,\ L\}$ indicates either the right (R) or left (L) leg, and the subscript $m \in \mathcal{M} \triangleq \{\text{glute}, \text{quad}, \text{ham}\}$ indicates muscle group. The uncertain functions Ω_m^s relate muscle stimulation intensity and the resulting torque about the joint that the muscle crosses and are modeled as [27]

$$\Omega_m^s \triangleq \lambda_m^s \eta_m^s \cos\left(a_m^s\right), \quad m \in \mathcal{M},\ s \in \mathcal{S}$$

where $\lambda_m^s \in \mathbb{R}$ denotes the uncertain moment arm of the muscle force about the joint, $\eta_m^s \in \mathbb{R}$ denotes the uncertain nonlinear function relating stimulation intensity to muscle fiber force, and $a_m^s \in \mathbb{R}$ denotes the uncertain pennation angle of the muscle fibers.

1) Property 1: The moment arms of the muscle groups about their respective joints λ_m^s, $\forall m \in \mathcal{M}$, $\forall s \in \mathcal{S}$ depend on the joint angles and are nonzero, continuously differentiable, and bounded with bounded first time derivatives [33].

2) Property 2: The functions relating stimulation voltage to muscle fiber force η_m^s, $\forall m \in \mathcal{M}$, $\forall s \in \mathcal{S}$ are functions of the force-length and force-velocity relationships of the muscle being stimulated and are lower and upper bounded by known positive constants $c_{\eta 1},\ c_{\eta 2} \in \mathbb{R}^+$, respectively, provided the muscle is not fully stretched [34] or contracting concentrically at its maximum shortening velocity.

3) Property 3: The muscle fiber pennation angles $a_m^s \neq (n\pi + \pi/2)$, $\forall m \in \mathcal{M}$, $\forall s \in \mathcal{S}$, $\forall n \in \mathbb{Z}$ (i.e., $\cos\left(a_m^s\right) \neq 0$) [35].

4) Property 4: Based on Properties 1–3, the functions relating voltage applied to the muscle groups and the resulting torques about the joints are nonzero and bounded. In other words, $0 < c_\omega < |\Omega_m^s| \leq c_\Omega$, $\forall m \in \mathcal{M}$, $\forall s \in \mathcal{S}$, where $c_\omega,\ c_\Omega \in \mathbb{R}_{>0}$ are known positive constants.

The Jacobian elements T_m^s are based on the joint torque transfer ratios $T_j^s \in \mathbb{R}$ [23], which are defined as

$$T_h^s \triangleq -\frac{\partial q_h^s}{\partial q}, \quad T_k^s \triangleq \frac{\partial q_h^s}{\partial q} + \frac{\partial q_k^s}{\partial q}, \quad s \in \mathcal{S}.$$

The subscript $j \in \mathcal{J} \triangleq \{h,\ k\}$ indicates hip (h) and knee (k) joints. From Assumption 1, the torque transfer ratios for the muscle groups, T_m^s, can then be determined, according to the joint that each muscle spans, as

$$T_{\text{glute}}^s = T_h^s, \quad T_{\text{quad}}^s = T_{\text{ham}}^s = T_k^s, \quad s \in \mathcal{S}.$$

The passive viscoelastic effects of the tissues surrounding the hip and knee joints, denoted by τ_p in (2), can be defined as

$$\tau_p \triangleq \sum_{j\in\mathcal{J}} \sum_{s\in\mathcal{S}} T_j^s \tau_{j,p}^s$$

where $\tau_{j,p}^s \in \mathbb{R}$ denotes resultant torques about the rider's joints from viscoelastic tissue forces, modeled as [36], [37]

$$\tau_{j,p}^s \triangleq k_{j,1}^s \exp\left(k_{j,2}^s \gamma_j^s\right)\left(\gamma_j^s - k_{j,3}^s\right) + b_{j,1}^s \tanh\left(-b_{j,2}^s \dot{\gamma}_j^s\right) - b_{j,3}^s \dot{\gamma}_j^s$$

for $j \in \mathcal{J}$, $s \in \mathcal{S}$, where $k_{j,i}^s,\ b_{j,i}^s \in \mathbb{R}$, $i \in \{1,\ 2,\ 3\}$, are unknown constant coefficients, and $\gamma_j^s \in \mathbb{R}$ denotes the relative hip and knee joint angles, defined as

$$\gamma_h^s \triangleq q_h^s - q_t + \pi, \quad \gamma_k^s \triangleq q_h^s - q_k^s, \quad s \in \mathcal{S}.$$

The equation of motion for the total cycle-rider system with electrical stimulation is obtained by substituting (2) and (3) into (1) as

$$M\ddot{q} + V\dot{q} + G - \tau_p - \tau_b - \tau_d = \sum_{s\in\mathcal{S}} \sum_{m\in\mathcal{M}} v_m^s \Omega_m^s T_m^s. \tag{4}$$

The model in (4) has the following properties.

5) Property 5: $c_m \leq M \leq c_M$, where $c_m,\ c_M \in \mathbb{R}_{>0}$ are known constants. *Property 6:* $|V| \leq c_V\,|\dot{q}|$, where $c_V \in \mathbb{R}_{>0}$ is a known constant. *Property 7:* $|G| \leq c_G$, where $c_G \in \mathbb{R}_{>0}$ is a known constant. *Property 8:* $|\tau_d| \leq c_d$, where $c_d \in \mathbb{R}_{>0}$ is a known constant. *Property 9:* $\left|T_j^s\right| \leq c_T\ \forall s \in \mathcal{S}$, $\forall j \in \mathcal{J}$, where $c_T \in \mathbb{R}_{>0}$ is a known constant. *Property 10:* $|\tau_p| \leq c_{P1} + c_{P2}\,|\dot{q}|$, where $c_{P1},\ c_{P2} \in \mathbb{R}_{>0}$ are known constants. *Property 11:* $(1/2)\dot{M} - V = 0$.

B. Switched System Model

1) Stimulation Pattern Development: The muscle torque transfer ratios T_m^s indicate how each muscle group should be activated to induce forward pedaling. Multiplying the joint torque yielded by a muscle contraction with T_m^s transforms that torque to a resultant torque about the crank. Therefore, if only forward pedaling is desired, then each muscle group should only be activated when it yields a clockwise (with respect to Fig. 1) torque about the crank. In other words, stimulation should only activate the quadriceps when T_{quad} is negative, the hamstrings when T_{ham} is positive, and the gluteal muscles when T_{glute} is positive. However, this stimulation pattern would require stimulation of the muscle groups for vanishingly small values of T_m^s (i.e., near the so-called dead points of the crank cycle) and may therefore activate the muscles inefficiently, in the sense that large values of stimulation and metabolic power output would result in little power output at the cycle crank. Therefore, to increase FES-cycling efficiency, motivation exists to only stimulate a muscle group when its torque transfer ratio is sufficiently large. Indeed, evidence in [23] suggests that the stimulation interval for each muscle group should be minimized to optimize metabolic efficiency. With these constraints, the stimulation intervals for each muscle group $\mathcal{Q}_m^s \subseteq \mathcal{Q}$ can be defined as

$$\mathcal{Q}_{\text{glute}}^s \triangleq \left\{q \in \mathcal{Q} \mid T_{\text{glute}}^s(q) > \varepsilon_{\text{glute}}^s\right\} \tag{5}$$

$$\mathcal{Q}_{\text{quad}}^s \triangleq \left\{q \in \mathcal{Q} \mid -T_{\text{quad}}^s(q) > \varepsilon_{\text{quad}}^s\right\} \tag{6}$$

$$\mathcal{Q}_{\text{ham}}^s \triangleq \left\{q \in \mathcal{Q} \mid T_{\text{ham}}^s(q) > \varepsilon_{\text{ham}}^s\right\} \tag{7}$$

where $\varepsilon_m^s \in \mathbb{R}_{>0}$ are selectable constants. Selection of ε_m^s indicates a user-defined minimum torque transfer ratio required before a muscle group may be activated, so that ε_m^s is inversely related to the length of a muscle group's stimulation interval. To ensure that $\mathcal{Q}_m^s \neq \emptyset$ for each m, it is required that $\varepsilon_{\text{glute}}^s < \max\left(T_{\text{glute}}^s\right)$, $\varepsilon_{\text{quad}}^s < \max\left(-T_{\text{quad}}^s\right)$, and $\varepsilon_{\text{ham}}^s < \max\left(T_{\text{ham}}^s\right)$. Denote the set $\mathcal{Q}_c \triangleq \cup_{s\in\mathcal{S}}\left(\cup_{m\in\mathcal{M}}\mathcal{Q}_m^s\right)$ as the controlled region, i.e., the portion of the crank cycle over which muscles are stimulated, and the set $\mathcal{Q}_u \triangleq \mathcal{Q}\backslash\mathcal{Q}_c$ as the uncontrolled region, i.e., the portion of the crank cycle over which no muscles are stimulated. Depending on the kinematic parameters of the cycle and rider, along with the selection of ε_m^s, $\mathcal{Q}_u$ may be empty, but the present development considers the general case where $\mathcal{Q}_u$ is not empty.

2) Switched Control Input: To stimulate the rider's muscle groups according to the stimulation pattern defined by (5)–(7), the stimulation input to each muscle must be switched on and off at appropriate points along the crank cycle. Based on this stimulation pattern, piecewise constant switching signals for each muscle group $\sigma_m^s \in \{0, 1\}$ can be defined as

$$\sigma_m^s \triangleq \begin{cases} 1, & \text{if } q \in \mathcal{Q}_m^s \\ 0, & \text{if } q \notin \mathcal{Q}_m^s \end{cases}, \quad m \in \mathcal{M},\ s \in \mathcal{S}. \tag{8}$$

Then, the stimulation intensity input to each muscle group v_m^s can be defined as

$$v_m^s \triangleq k_m^s \sigma_m^s u, \quad m \in \mathcal{M},\ s \in \mathcal{S} \tag{9}$$

where $u \in \mathbb{R}$ is the subsequently designed control input, and $k_m^s \in \mathbb{R}_{>0}$ are control gains that can be tuned to compensate for the relative strength and effectiveness of each muscle group. Substituting (8) and (9) into (4) yields the following switched system:

$$M\ddot{q} + V\dot{q} + G - \tau_p - \tau_b - \tau_d = \begin{cases} Bu, & \text{if } q \in \mathcal{Q}_c \\ 0, & \text{if } q \in \mathcal{Q}_u \end{cases} \tag{10}$$

where $B \in \mathbb{R}$ is the discontinuous control effectiveness term, defined as

$$B \triangleq \sum_{s\in\mathcal{S}} \sum_{m\in\mathcal{M}} k_m^s \sigma_m^s \Omega_m^s T_m^s. \tag{11}$$

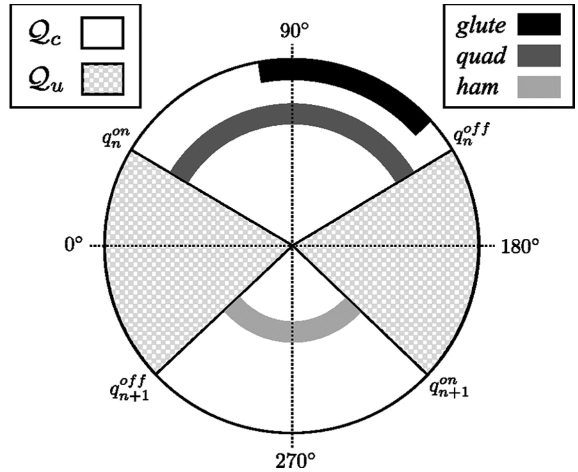

Fig. 2. Example stimulation pattern depicting intervals of the crank cycle over which the quadriceps femoris (quad), hamstrings (ham), and gluteal (glute) muscle groups of one leg are stimulated. The crank positions q_n^{on} and q_n^{off} denote the points at which the crank exits or enters, respectively, the uncontrolled region $\mathcal{Q}_u$.

Property 4 and (5)–(8) can be used to demonstrate that B is zero if and only if the crank is in the uncontrolled region (i.e., $q \in \mathcal{Q}_u \Leftrightarrow B = 0$). In the controlled regions, B can be bounded as

$$c_{B1} \leq B \leq c_{B2}, \quad q \in \mathcal{Q}_c, \tag{12}$$

where $c_{B1},\ c_{B2} \in \mathbb{R}_{>0}$ are known constants.

3) Switching States and Times: Assuming that the initial crank angle q_0^{on} is an element of $\mathcal{Q}_c$, the known sequence of switching states, which are precisely the limit points of $\mathcal{Q}_u$, is defined as $\left\{q_n^{\text{on}},\ q_n^{\text{off}}\right\}$, $n \in \{0,\ 1,\ 2,\ \ldots\}$, where the superscripts on and off indicate that the sum of signals σ_m^s is switching from zero to nonzero or nonzero to zero, respectively. The corresponding sequence of unknown switching times $\left\{t_n^{\text{on}},\ t_n^{\text{off}}\right\}$ is defined such that each on-time t_n^{on} and off-time t_n^{off} denotes the instant when q reaches the corresponding on-angle q_n^{on} and off-angle q_n^{off}, respectively. Fig. 2 exemplifies the stimulation pattern and the associated switching states.

III. Control Development

Based on the model in (1), a robust controller is subsequently developed to ensure cadence tracking. The controller does not depend explicitly on the model, as the model is uncertain, but the structure of the model motivates the control design. Only the torque transfer ratios T_m^s, which depend on the measurable rider's limb lengths and seat position, must be known to determine which muscle group should be stimulated throughout the crank cycle. Known bounds on the other model parameters enable the robust controller to guarantee tracking despite model uncertainty.

The control objective is to track a desired crank cadence with performance quantified by the tracking error signal $r \in \mathbb{R}$, defined as

$$r \triangleq \dot{q}_d - \dot{q} \tag{13}$$

where $q_d \in \mathbb{R}$ denotes the desired crank position, designed so that its derivatives exist and $\dot{q}_d,\ \ddot{q}_d \in \mathcal{L}_\infty$. Without loss of generality, q_d is designed to monotonically increase, i.e., backpedaling is not desired.

Taking the time derivative of (13), multiplying by M, and using (10) and (13) yields the open-loop error system

$$M\dot{r} = \chi - Vr - \begin{cases} Bu, & \text{if } q \in \mathcal{Q}_c \\ 0, & \text{if } q \in \mathcal{Q}_u \end{cases} \tag{14}$$

where the auxiliary term $\chi \in \mathbb{R}$ is defined as

$$\chi \triangleq M\ddot{q}_d + V\dot{q}_d + G - \tau_p - \tau_b - \tau_d. \tag{15}$$

Based on (15) and Properties 5–10, χ can be bounded as

$$|\chi| \leq c_1 + c_2 |r| \tag{16}$$

where $c_1,\ c_2 \in \mathbb{R}_{>0}$ are known constants.

Based on (14) and the subsequent stability analysis, the control input is designed as

$$u \triangleq k_1 r + k_2 \mathrm{sgn}(r) \tag{17}$$

where $\mathrm{sgn}(\cdot)$ denotes the signum function, and $k_1,\ k_2 \in \mathbb{R}_{>0}$ are constant control gains. After substituting (17) into the open-loop error system in (14), the following switched closed-loop error system is obtained:

$$M\dot{r} = \chi - Vr - \begin{cases} B\left[k_1 r + k_2 \mathrm{sgn}(r)\right], & \text{if } q \in \mathcal{Q}_c \\ 0, & \text{if } q \in \mathcal{Q}_u \end{cases}. \tag{18}$$

IV. Stability Analysis

Let $V_L : \mathbb{R} \to \mathbb{R}$ be a positive definite, continuously differentiable, common Lyapunov-like function defined as

$$V_L \triangleq \frac{1}{2} M r^2. \tag{19}$$

The common Lyapunov-like function V_L is radially unbounded and satisfies the following inequalities:

$$\left(\frac{c_m}{2}\right) r^2 \leq V_L \leq \left(\frac{c_M}{2}\right) r^2. \tag{20}$$

Theorem 1: For $q \in \mathcal{Q}_c$, the closed-loop error system in (18) is exponentially stable in the sense that

$$|r(t)| \leq \sqrt{\frac{c_M}{c_m}}\, \left|r\left(t_n^{\mathrm{on}}\right)\right| \exp\left[-\frac{\lambda_c}{2}\left(t - t_n^{\mathrm{on}}\right)\right] \tag{21}$$

for all $t \in \left(t_n^{\mathrm{on}},\ t_n^{\mathrm{off}}\right)$ and for all n, where $\lambda_c \in \mathbb{R}_{>0}$ is defined as

$$\lambda_c \triangleq \frac{2}{c_M}\left(k_1 c_{B1} - c_2\right) \tag{22}$$

provided the following sufficient gain conditions are satisfied:

$$k_1 > \frac{c_2}{c_{B1}}, \quad k_2 \geq \frac{c_1}{c_{B1}}. \tag{23}$$

Proof: It can be demonstrated that the time derivative of (19) exists almost everywhere (a.e.), i.e., for almost all $t \in \left(t_n^{\mathrm{on}},\ t_n^{\mathrm{off}}\right)$, and, after substituting (18), can be upper bounded using (12) and (16) as

$$\dot{V}_L \overset{a.e.}{\leq} -\left(k_2 c_{B1} - c_1\right)|r| - \left(k_1 c_{B1} - c_2\right) r^2. \tag{24}$$

From (12), it can be demonstrated that the inequality in (24) holds for all subsets $\mathcal{Q}_m^s$ of the controlled region $\mathcal{Q}_c$, so it can be concluded that V_L is a common Lyapunov-like function in the controlled region. Provided the conditions on the control gains in (23) are satisfied, (20) can be used to upper bound (24) as

$$\dot{V}_L \overset{a.e.}{\leq} -\lambda_c V_L \tag{25}$$

where λ_c was defined in (22). The inequality in (25) can be solved to yield

$$V_L(t) \leq V_L\left(t_n^{\mathrm{on}}\right) \exp\left[-\lambda_c\left(t - t_n^{\mathrm{on}}\right)\right] \tag{26}$$

for all $t \in \left(t_n^{\mathrm{on}},\ t_n^{\mathrm{off}}\right)$ and for all n. Rewriting (26) using (20) and performing some algebraic manipulation yields (21). ■

Remark 1: Theorem 1 guarantees that the desired cadence can be tracked with exponential convergence, provided that the crank angle does not exit the controlled region. Thus, if the stimulation pattern and desired cadence are designed such that the crank is not required to exit the controlled region, the controller in (17) may yield exponential tracking for all time. If the desired cadence is designed such that the crank must exit the controlled region, the system may become uncontrolled and the following theorem details the resulting error system behavior.

Theorem 2: For $q \in \mathcal{Q}_u$, the closed-loop error system in (18) can be bounded as

$$|r(t)| \leq \left\{\frac{c_M}{c_m} r^2\left(t_n^{\mathrm{off}}\right) \exp\left[\lambda_u\left(t - t_n^{\mathrm{off}}\right)\right] + \frac{1}{c_m}\exp\left[\lambda_u\left(t - t_n^{\mathrm{off}}\right)\right] - \frac{1}{c_m}\right\}^{1/2} \tag{27}$$

for all $t \in \left[t_n^{\mathrm{off}},\ t_{n+1}^{\mathrm{on}}\right]$ and for all n.

Proof: In the uncontrolled region, the time derivative of (19) can be expressed using (18) and Property 5 as

$$\dot{V}_L = \chi r$$

which can be upper bounded using (16) and (20) as

$$\dot{V}_L \leq \lambda_u \left(V_L + \frac{1}{2}\right). \tag{28}$$

The solution to (28) over the interval $t \in \left[t_n^{\mathrm{off}},\ t_{n+1}^{\mathrm{on}}\right]$ yields the following upper bound on V_L in the uncontrolled region:

$$V_L(t) \leq V_L\left(t_n^{\mathrm{off}}\right) \exp\left[\lambda_u\left(t - t_n^{\mathrm{off}}\right)\right] + \frac{1}{2}\left\{\exp\left[\lambda_u\left(t - t_n^{\mathrm{off}}\right)\right] - 1\right\} \tag{29}$$

for all $t \in \left[t_n^{\mathrm{off}},\ t_{n+1}^{\mathrm{on}}\right]$ and for all n. Rewriting (29) using (20) and performing some algebraic manipulation yields (27). ■

Remark 2: The exponential bound in (27) indicates that in the uncontrolled regions, the error norm is bounded by an exponentially increasing envelope. Since the error norm decays at an exponential rate in the controlled regions, as described by (21), sufficient conditions for stability of the overall system can be developed based on the exponential time constants λ_c and λ_u and the time that the crank dwells in each region (dwell times) $\Delta t_n^{\mathrm{on}} \triangleq t_n^{\mathrm{off}} - t_n^{\mathrm{on}}$ and $\Delta t_n^{\mathrm{off}} \triangleq t_{n+1}^{\mathrm{on}} - t_n^{\mathrm{off}}$. However, a challenge is that the dwell time Δt_n^{on} and reverse dwell time $\Delta t_n^{\mathrm{off}}$ (nomenclature derived from [38]) depend on the switching times, which are unknown *a priori*. The following assumption introduces bounds on the uncertain dwell times.

Assumption 2: The dwell times Δt_n^{on} and Δt_n^{off} have known, constant bounds for all n such that

$$\Delta t_n^{\text{on}} \geq \Delta t_{min}^{\text{on}}, \quad \Delta t_n^{\text{off}} \leq \Delta t_{\max}^{\text{off}}.$$

This assumption is reasonable in the sense that the dwell time in the controlled and uncontrolled regions will have lower and upper bounds, respectively, provided the cadence remains within predefined limits, and during FES-cycling it is common to impose such limits for safety reasons.

Remark 3: With known bounds on the time between switches and known rates of convergence and divergence of the tracking error, a known ultimate bound on the tracking error can be calculated. Theorem 3 gives the value of this ultimate bound along with a sufficient condition for convergence of the tracking error to that bound.

Theorem 3: The closed-loop error system in (18) is ultimately bounded in the sense that $|r(t)|$ converges to a ball with constant radius $d \in \mathbb{R}_{>0}$ as the number of crank cycles approaches infinity (i.e., as $n \to \infty$), where d is defined as

$$d \triangleq \sqrt{\frac{2b}{c_m(1-a)}} \tag{30}$$

and $a, \ b \in \mathbb{R}_{\geq 0}$ are defined as

$$a \triangleq \exp\left(\lambda_u \Delta t_{\max}^{\text{off}} - \lambda_c \Delta t_{\min}^{\text{on}}\right)$$
$$b \triangleq \frac{1}{2}\left[\exp\left(\lambda_u \Delta t_{\max}^{\text{off}}\right) - 1\right]$$

provided the following condition is satisfied:

$$\lambda_c > \lambda_u \frac{\Delta t_{\max}^{\text{off}}}{\Delta t_{\min}^{\text{on}}}. \tag{31}$$

Proof: Using (26) and (29) sequentially and assuming the worst case scenario for each cycle where $\Delta t_n^{\text{on}} = \Delta t_{\min}^{\text{on}}$ and $\Delta t_n^{\text{off}} = \Delta t_{\max}^{\text{off}}$, an upper bound for $V_L(t_n^{\text{on}})$ after N cycles can be developed as

$$V_L\left(t_N^{\text{on}}\right) \leq V_L\left(t_0^{\text{on}}\right) a^N + b \sum_{n=0}^{N-1} a^n \tag{32}$$

where $N \in \mathbb{N}_{>0}$. The sequence $\{V_L(t_n^{\text{on}})\}$ is positive, monotonic, and bounded, provided (31) is satisfied (i.e., $a < 1$); therefore, the limit of $\{V_L(t_n^{\text{on}})\}$ exists and can be expressed as

$$\lim_{n \to \infty} V_L\left(t_n^{\text{on}}\right) = \overline{d}$$

where $\overline{d} \in \mathbb{R}_{>0}$ is a known constant defined as

$$\overline{d} \triangleq \frac{b}{1-a}. \tag{33}$$

Therefore, $V_L(t_n^{\text{on}})$ is ultimately bounded by $\overline{d}$ in the sense that as $n \to \infty, \ V_L(t_n^{\text{on}}) \to \overline{d}$. Monotonicity of the bounds in (26) and (29) can be used to demonstrate that $V_L(t)$ is ultimately bounded by $\overline{d}$. Using (20), it can then be demonstrated that as $n \to \infty$, $|r(t)|$ converges to a ball with constant radius d, where d was defined in (30), in the sense that $|r(t \geq t_d)| \leq d$ for some time $t_d \in [0, \ \infty)$. ■

V. Experiments

FES-cycling experiments were conducted with the primary objective of evaluating the performance of the switched controller given in (17) and distributed to the gluteal, quadriceps femoris, and hamstrings muscle groups according to (9). The experiments were divided into Protocols A and B. The objective of both protocols was to demonstrate the controller's cadence tracking performance in the presence of parametric uncertainty and unmodeled disturbances. The FES-cycling trials were stopped if the control input saturated, the subject reported significant discomfort, the cadence fell below 0 RPM, the trial runtime expired, or the cadence exceeded 60 rpm. The experiments could also be ended at any time by the subjects via an emergency stop switch.

A. Subjects

Four able-bodied male subjects 25–27 years old were recruited from the student population at the University of Florida, and one male subject with PD, 60 years old, with a modified Hoehn and Yahr disability score of 2.5 [39], was recruited from the University of Florida Center for Movement Disorders and Neurorestoration. Each subject gave written informed consent approved by the University of Florida Institutional Review Board. Able-bodied subjects were recruited to validate the controller design, and the subject with PD was recruited to demonstrate feasibility of the proposed approach in a potential patient population.

The subject with PD in this experiment exhibited mild bilateral motor impairment with evident tremor. It was observed during preliminary testing that the subject's right side was more affected (i.e., greater tremor) and exhibited bradykinesia during cycling (i.e., when the right leg was supposed to pedal, cadence decreased significantly). In addition, preliminary testing revealed that subject could not tolerate the level of stimulation intensity necessary for FES-induced cycling (i.e., FES-cycling without volitional effort from the rider). It was hypothesized that FES-assisted cycling (i.e., FES-cycling with volitional effort from the rider) would be a more appropriate protocol for subjects with PD. It was further hypothesized that FES-assistance would provide sensory cues and muscle activation assistance during cycling and thereby decrease variability in the subject's cadence.

B. FES-Cycling Test Bed

A commercially available, stationary, recumbent exercise cycle (AudioRider R400, NordicTrack) was modified for the purposes of the FES-cycling experiments. The cycle originally had a flywheel which was driven by a freewheel. The freewheel was then replaced with a fixed gear so that the crankshaft was directly coupled to the flywheel, allowing the flywheel to contribute its momentum to the cycle-rider momentum and improving the system energetics [40]. The cycle has an adjustable seat and a magnetic hysteresis brake on the flywheel with 16 incremental levels of resistance (resistance was set to Level 1 unless otherwise noted). Custom pedals were constructed that allowed high-top orthotic boots (Rebound Air Walker, Össur) to be affixed to them; these orthotic pedals served to fix the rider's feet to the pedals, prevent dorsiflexion and plantarflexion of the ankles, and maintain sagittal alignment of the lower legs. An optical, incremental encoder (HS35F, BEI Sensors, resolution 0.018°) was added to the cycle and coupled to the crank shaft to measure the cycling cadence. The cycle was equipped with a Hall effect sensor and magnet on the crank that provided an absolute position reference once per cycle.

A current-controlled stimulator (RehaStim, Hasomed) delivered biphasic, symmetric, rectangular pulses to the subject's muscle groups via bipolar, self-adhesive electrodes (PALS 3 × 5).[2] A personal computer equipped with data acquisition hardware and software was used to read the encoder signal, calculate the control input, and command the stimulator. Stimulation frequency was fixed at 60 Hz to leverage the results found in [41]. Stimulation intensity was controlled by fixing the pulse amplitude for each muscle group and controlling the pulsewidth according to (17). Pulse amplitude was determined for each subject's muscle groups in preliminary testing and ranged from 50–110 mA.

C. Experimental Setup

Electrodes were placed over the subjects' gluteal, quadriceps femoris, and hamstrings muscle groups, according to Axelgaard's electrode placement manual,[3] while subjects were standing upright. Subjects were then seated on the stationary cycle, and their feet were inserted securely into the orthotic pedals. The cycle seat position was adjusted for each subject's comfort while ensuring that hyperextension of the knees could not be achieved while cycling. The subject's hip position relative to the cycle crank axis was measured along with the distances between the subjects' greater trochanters and lateral femoral condyles (l_t) and between the subjects' lateral femoral condyles and the pedal axes of rotation (l_l). These distances were used to calculate the torque transfer ratios for the subjects' muscle groups and to thereby determine the stimulation pattern.

The desired crank velocity was defined in radians per second as

$$\dot{q}_d \triangleq \frac{5\pi}{3}\left[1 - \exp\left(-\phi t\right)\right] \tag{34}$$

where $\phi \in \mathbb{R}_{>0}$ was a selectable constant used to control the acceleration of the desired trajectory and $t_0^{\text{on}} = 0$ seconds. The trajectory in (34) ensured that the desired velocity started at zero revolutions per minute (RPM) and smoothly approached 50 rpm. The control gains, introduced in (9) and (17), were tuned to yield acceptable tracking performance for each subject in preliminary testing and ranged as follows: $k_1 \in [70,\ 150]$, $k_2 \in [7,\ 15]$, $k^s_{\text{glute}} \in [0.5625,\ 1.125]$, $k^s_{\text{quad}} \in [0.9,\ 1.125]$, $k^s_{\text{ham}} \in [0.816,\ 1.2375]$, $\forall s \in \mathcal{S}$.

D. Protocol A

Protocol A was completed by all able-bodied subjects and consisted of a voluntary cycling phase followed by five minutes of rest and a subsequent FES-cycling phase. During the voluntary cycling phase, subjects were shown a computer screen with a real-time plot of their actual cadence, as measured by the encoder, versus the desired cadence given in (34), and each subject was asked to voluntarily pedal so that the two plots coincided with one another (i.e., minimize the tracking error r). After 175 seconds had elapsed, the flywheel resistance was increased from Level 1 directly to Level 9 for a period of 30 seconds, after which the resistance was decreased back to Level 1 for the remainder of the cycling phase. The voluntary cycling phase lasted five minutes.

Following five minutes of rest, the FES-cycling phase was initiated, wherein cycling was only controlled by stimulation of the gluteal, quadriceps femoris, and hamstrings muscle groups (i.e., a completely passive rider). The stimulation pattern (i.e., the range of crank angles over which each muscle was stimulated) for Protocol A was defined by selecting $\varepsilon_{\text{glute}} = 0.2$, $\varepsilon_{\text{quad}} = 0.3$, $\varepsilon_{\text{ham}} = 0.38$, which was found to yield satisfactory performance in preliminary testing. While the same values of ε_m were used for all subjects, the stimulation pattern resulting from the choice of each ε_m was slightly different for each subject because each subject had different leg lengths and preferred seating positions. The subjects' limbs were then positioned manually so that the initial crank position was in the controlled region, and then the controller was activated. The subjects were instructed to relax as much as possible throughout this phase and to make no effort to voluntarily control the cycling motion; additionally, the subjects were not given any indication of the control performance (i.e., subjects could no longer see the actual or desired trajectory). As in the voluntary cycling phase, the flywheel resistance was increased from Level 1 to Level 9 for $t \in [175,\ 205]$ seconds to demonstrate the controller's robustness to an unknown, bounded, time-varying disturbance. The FES-cycling phase lasted five minutes.

E. Protocol B

Protocol B was completed by the subject with PD and was the same as Protocol A, with the exception that the subject was allowed to voluntarily pedal during the FES-cycling phase (i.e., FES-assisted cycling) and could see the actual and desired cadence. While Protocol A was intended to demonstrate the controller's performance with a completely passive rider, as would be the case with a subject with motor complete spinal cord injury, Protocol B demonstrates feasibility of the developed controller for a broader patient population with intact, albeit diminished, motor control, such as those with incomplete spinal cord injury, hemiparetic stroke, traumatic brain injury, and PD. From an analytical perspective, voluntary assistance from the rider can be viewed as an unmodeled disturbance and so can be lumped into τ_d in (10). Although disturbances are generally neither assistive nor resistive, voluntary effort from the rider during FES-cycling is generally assistive and is therefore expected to decrease the control input needed to track the desired cadence.

F. Results

1) Protocol A Results: Fig. 3 depicts one able-bodied subject's tracking performance, quantified by the cadence tracking error r, and the stimulation intensity (pulsewidth) input to each muscle group v^s_m during the FES-cycling phase of Protocol A, and Fig. 4 provides an enhanced view of the control input over a single crank cycle to illustrate the controller switching

[2]Surface electrodes for this study were provided compliments of Axelgaard Manufacturing Co., Ltd.

[3]http://www.palsclinicalsupport.com/videoElements/videoPage.php

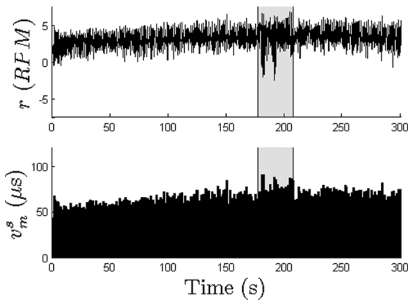

Fig. 3. One subject's cadence tracking error r (top) and control input v_m^s to each muscle group (bottom) during the FES-cycling trial of Protocol A. The subject was instructed to relax completely while the quadriceps femoris, hamstrings, and gluteal muscle groups were stimulated to achieve cycling at the desired cadence. Shaded regions mark the period during which the ergometer's resistance was increased to Level 9.

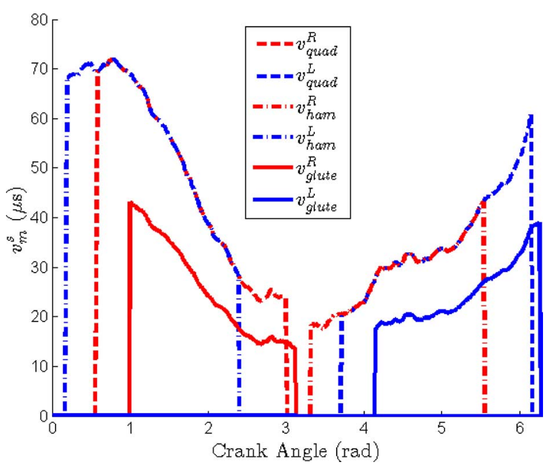

Fig. 4. Control input over a single crank cycle illustrating the switching of the controller in (17) between the quadriceps femoris, hamstrings, and gluteal muscle groups according to (9) during the FES-cycling trial of Protocol A for Subject AB3.

and distribution of the control input across the muscle groups. Table I compares the subjects' volitional and FES-induced tracking performance, quantified by the mean and standard deviation of the cadence tracking error in RPM, over the total trial ($t \in [0,\ 300]$ seconds) and during several phases of each trial: the transient phase ($t \in [0,\ 40]$ seconds), the steady state phase ($t \in (40,\ 175)$ seconds), the added disturbance phase ($t \in [175,\ 205]$ seconds), and the final phase ($t \in (205,\ 300]$ seconds). Fig. 5 compares another subject's cadence tracking error in the voluntary and FES-induced cycling phases. All trials went to completion.

2) Protocol B Results: Fig. 6 depicts the tracking performance of the subject with PD, quantified by the cadence tracking error r, and the stimulation intensity (pulsewidth) input to each muscle group v_m^s during the FES-assisted phase of Protocol B. An enhanced view of the control input over a single crank cycle is provided in Fig. 7 to illustrate the controller switching and distribution of the control input across the muscle groups. Table II summarizes the volitional and FES-assisted cadence tracking performance of the subject with PD using the same metrics as described in Section V-F1. Fig. 8 compares the subject's cadence tracking error in the voluntary and FES-assisted cycling phases. All trials went to completion.

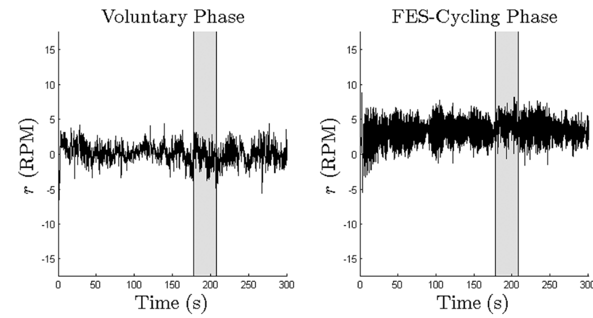

Fig. 5. Cadence tracking error r for the voluntary (left) and FES-cycling (right) phases of Protocol A for Subject AB3. During voluntary cycling, the subject was shown a plot of the desired and actual cadence on a monitor and was asked to pedal so that the difference was minimized, and no stimulation was applied. During FES-cycling, the subject was instructed to relax and had no indication of tracking performance while FES was applied to the lower limb muscles to induce cycling. Shaded regions mark the period during which the ergometer's resistance was increased to Level 9.

TABLE I
COMPARISON OF CADENCE TRACKING ERROR IN RPM (mean ± standard deviation) FOR ALL ABLE-BODIED SUBJECTS' VOLITIONAL AND FES-CYCLING OVER TOTAL TRIAL AND DURING TRANSIENT, STEADY STATE, DISTURBANCE, AND FINAL PHASES

Subject	Phase	Volitional Error (RPM)	FES Error (RPM)
AB1	Transient	1.04±1.58	2.41±1.08
	Steady State	-0.06±1.59	3.12±1.04
	Disturbance	0.04±2.01	3.39±1.61
	Final	-0.43±1.70	3.47±1.21
	Total Trial	-0.02±1.73	3.16±1.22
AB2	Transient	0.28±3.26	6.03±2.07
	Steady State	-0.07±1.15	9.78±1.58
	Disturbance	0.01±1.43	14.56±1.78
	Final	-0.01±1.17	12.68±1.21
	Total Trial	0.01±1.63	10.68±2.92
AB3	Transient	0.62±1.68	2.31±2.54
	Steady State	0.01±1.06	3.12±1.70
	Disturbance	-0.21±1.51	4.14±1.52
	Final	-0.31±1.38	3.19±1.63
	Total Trial	-0.03±1.34	3.14±1.85
AB4	Transient	1.22±2.72	3.51±2.75
	Steady State	-0.01±1.36	3.93±1.78
	Disturbance	0.40±1.56	4.74±3.52
	Final	0.18±1.34	4.41±2.97
	Total Trial	0.25±1.67	4.11±2.57
All	Transient	0.79±2.31	3.56±2.11
	Steady State	-0.03±1.29	4.99±1.53
	Disturbance	0.06±1.63	6.71±2.11
	Final	-0.14±1.40	5.94±1.76
	Total Trial	0.05±1.59	5.27±2.14

G. Discussion

The results of Protocol A successfully demonstrate the ability of the controller in (17), distributed across the muscle groups according to (9), to achieve ultimately bounded tracking of the desired cadence despite parametric uncertainty (e.g., uncertain rider limb mass) and unknown disturbances. Ultimately bounded tracking was achieved even across a range of stimulation patterns. Although the ultimate bound on the tracking error

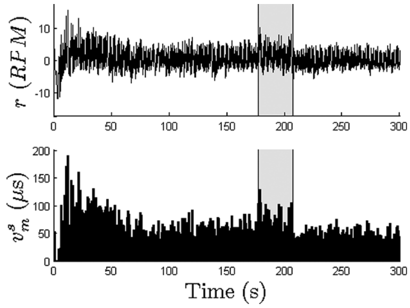

Fig. 6. Cadence tracking error r (top) and control input v_m^s to each muscle group (bottom) during the FES-assisted phase of Protocol B. The subject with PD was shown a plot of the desired and actual cadence on a monitor and was asked to pedal so that the difference was minimized, and FES was applied to the quadriceps femoris, hamstrings, and gluteal muscle groups to assist the subject in tracking the desired cadence. Shaded regions mark the period during which the ergometer's resistance was increased to Level 9.

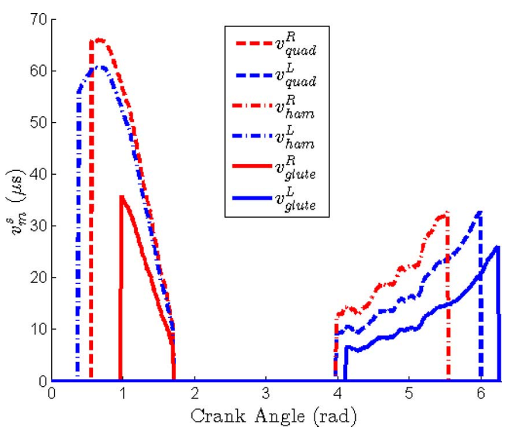

Fig. 7. Control input over a single crank cycle illustrating the switching of the controller in (17) between muscle groups according to (9) during the FES-assisted cycling trial of Protocol B. Through tuning of the control gains, the stimulation was biased towards the subject's right limb, which exhibited slowness of movement caused by PD.

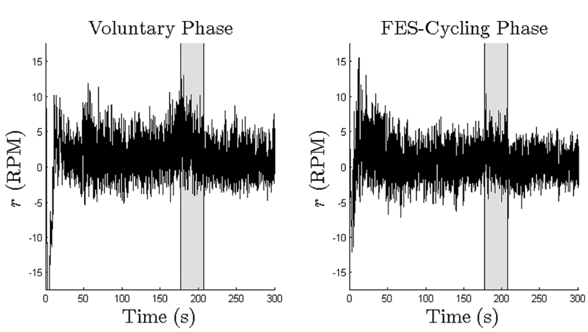

Fig. 8. Cadence tracking error r of the subject with PD during the voluntary (left) and FES-assisted (right) phases of Protocol B. During voluntary cycling, the subject was shown a plot of the desired and actual cadence on a monitor and was asked to pedal so that the difference was minimized, and no stimulation was applied. During FES-assisted cycling, the subject pedaled volitionally in the same manner as the previous trial, but stimulation was applied to assist in tracking the desired cadence. Shaded regions mark the period during which the ergometer's resistance was increased to Level 9.

was higher for FES-cycling than volitional cycling by all subjects in Protocol A, this was likely due to the steady state offset in the tracking error and not due to large variations in cycling cadence, as quantified in Table I. The cadence tracking error

TABLE II
COMPARISON OF CADENCE TRACKING ERROR IN RPM (mean $\pm$ standard deviation) OF SUBJECT WITH PD DURING VOLITIONAL AND FES-ASSISTED CYCLING OVER TOTAL TRIAL AND DURING TRANSIENT, STEADY STATE, DISTURBANCE, AND FINAL PHASES

Subject	Phase	Volitional Error (RPM)	FES Error (RPM)
PD	Transient	-1.28±7.41	1.28±4.87
	Steady State	0.80±3.21	0.07±2.82
	Disturbance	2.10±3.88	1.15±2.91
	Final	0.11±2.65	-0.46±2.32
	Total Trial	0.43±4.06	0.17±3.11

of all able-bodied subjects during voluntary and FES-induced cycling was 0.05± 1.59 rpm and 5.27±2.14 rpm, respectively. The steady state error observed in the FES-cycling phase may be caused by a lack of adaptation in the FES-cycling controller. During volitional cycling, riders can learn how to modulate the force output of the muscles involved in cycling to improve tracking performance over time. Therefore, to achieve cadence tracking performance during FES-cycling that is similar to that observed during volitional cycling, motivation arises to use adaptive control methods during the controlled regions. However, this is challenging because adaptive control methods usually only achieve asymptotic convergence of the tracking error, but stability of a switched system with stable and unstable subsystems can only be guaranteed if the convergence and divergence rates are known (as is the case with exponential convergence, for example).

The results of Protocol B demonstrate the controller's tracking performance despite the presence of an additional unknown disturbance (manifested as volitional effort from the subject with PD). The data given in Table II indicate that the addition of FES-assistance to the subject's volitional effort improved cadence tracking performance measurably (60.5% and 23.4% improvement in mean and standard deviation of the cadence tracking error across the total trial). The improvement in tracking performance may be due to the bias of the stimulation input towards the subject's affected right leg (as depicted in Fig. 7), providing both assistance in activating the appropriate muscle groups and a sensory cue to volitionally pedal faster. More data is needed to determine if these results are statistically significant, but the results nonetheless indicate the potential of FES-assistance to improve the ability of a person with PD to pedal at a desired cadence.

VI. CONCLUSION

An uncertain, nonlinear, time-varying model of a human rider pedaling a stationary cycle by means of FES was developed, and a stimulation pattern for the gluteal, quadriceps femoris, and hamstrings muscle groups was developed based on the system's Jacobian elements. The stimulation pattern, defined in (5)–(7), was used to distribute the stimulation control input to the muscle groups, switching the muscle groups on and off according to the crank angle. Therefore, the system was further modeled as a switched control system with autonomous, state-dependent switching with uncertain switching times. A common Lyapunov-like function was used to prove that the developed controller, given in (17), yields ultimately bounded tracking of a desired cadence (i.e., crank velocity), provided the desired cadence, control gains, and stimulation pattern satisfy sufficient conditions. The stability result and the developed sufficient conditions exploited the fact that the applied controller yields exponential stability in the controlled regions. Adaptive and learning-based controllers may yield advantages, but these methods typically yield asymptotic convergence. Therefore, future efforts will explore new analysis methods that allow for asymptotic controllers to be included in the switching design.

Experiments were conducted on four able-bodied subjects, and the results both demonstrate the robustness and stability of the developed switched controller. Experiments were also conducted on one subject with PD, and the results suggest that FES-assisted cycling using the developed switched controller may improve the ability of people with PD to track a desired cadence. While these results show promise, significant additional testing beyond the scope of this paper is needed to determine clinical efficacy. Specifically, different disease and injury populations will potentially respond differently to electrical stimulation, and disease-specific clinical trials will shed light on clinical impact. Within such studies, further opportunity exists to investigate comparisons of the developed Jacobian-based switching method to current rehabilitative devices.

ACKNOWLEDGMENT

Any opinions, findings and conclusions or recommendations expressed in this material are those of the authors and do not necessarily reflect the views of the sponsoring agency.

REFERENCES

[1] C. A. Phillips, J. S. Petrofsky, D. M. Hendershot, and D. Stafford, "Functional electrical exercise: A comprehensive approach for physical conditioning of the spinal cord injured patient," *Orthopedics*, vol. 7, no. 7, pp. 1112–1123, 1984.

[2] C.-W. Peng, S.-C. Chen, C.-H. Lai, C.-J. Chen, C.-C. Chen, J. Mizrahi, and Y. Handa, "Review: Clinical benefits of functional electrical stimulation cycling exercise for subjects with central neurological impairments," *J. Med. Biol. Eng.*, vol. 31, pp. 1–11, 2011.

[3] J. S. Petrofsky, H. Heaton, and C. A. Phillips, "Outdoor bicycle for exercise in paraplegics and quadriplegics," *J. Biomed. Eng.*, vol. 5, pp. 292–296, Oct. 1983.

[4] D. J. Pons, C. L. Vaughan, and G. G. Jaros, "Cycling device powered by the electrically stimulated muscles of paraplegics," *Med. Biol. Eng. Comput.*, vol. 27, no. 1, pp. 1–7, 1989.

[5] J. S. Petrofsky and J. Smith, "Three-wheel cycle ergometer for use by men and women with paralysis," *Med. Biol. Eng. Comput.*, vol. 30, pp. 364–369, 1992.

[6] M. Gföhler, M. Loicht, and P. Lugner, "Exercise tricycle for paraplegics," *Med. Biol. Eng. Comput.*, vol. 36, pp. 118–121, 1998.

[7] T. A. Perkins, N. N. Donaldson, N. A. C. Hatcher, I. D. Swain, and D. E. Wood, "Control of leg-powered paraplegic cycling using stimulation of the lumbro-sacral anterior spinal nerve roots," *IEEE Trans. Neural Syst. Rehabil. Eng.*, vol. 10, no. 3, pp. 158–164, Sep. 2002.

[8] K. J. Hunt, B. Stone, N.-O. Negård, T. Schauer, M. H. Fraser, A. J. Cathcart, C. Ferrario, S. A. Ward, and S. Grant, "Control strategies for integration of electric motor assist and functional electrical stimulation in paraplegic cycling: Utility for exercise testing and mobile cycling," *IEEE Trans. Neural Syst. Rehabil. Eng.*, vol. 12, no. 1, pp. 89–101, Mar. 2004.

[9] T. Watanabe, T. Murakami, and Y. Handa, "Preliminary tests of a prototype FES control system for cycling wheelchair rehabilitation," in *Proc. 13th Int. Conf. IEEE ICORR*, Jun. 2013, pp. 1–6.

[10] L. M. Schutte, M. M. Rodgers, F. E. Zajac, and R. M. Glaser, "Improving the efficacy of electrical stimulation-induced leg cycle ergometry: An analysis based on a dynamic musculoskeletal model," *IEEE Trans. Rehabil. Eng.*, vol. 1, no. 2, pp. 109–125, Jun. 1993.

[11] M. Gföhler, T. Angeli, T. Eberharter, P. Lugner, W. Mayr, and C. Hofer, "Test bed with force-measuring crank for static and dynamic investigation on cycling by means of functional electrical stimulation," *IEEE Trans. Neural Syst. Rehabil. Eng.*, vol. 9, no. 2, pp. 169–180, Jun. 2001.

[12] J. S. Petrofsky, "New algorithm to control a cycle ergometer using electrical stimulation," *Med. Biol. Eng. Comput.*, vol. 41, no. 1, pp. 18–27, Jan. 2003.

[13] K. J. Hunt, M. Rothe, T. Schauer, A. Ronchi, and N. O. Negåard, "Automatic speed control in FES cycling," in *Proc. 6th Conf. IFESS*, 2001, pp. 300–302.

[14] E. Ambrosini, S. Ferrante, T. Schauer, G. Ferrigno, F. Molteni, and A. Pedrocchi, "Design of a symmetry controller for cycling induced by electrical stimulation: Preliminary results on post-acute stroke patients," *Artif. Organs*, vol. 34, no. 8, pp. 663–667, Aug. 2010.

[15] J.-J. J. Chen, N.-Y. Yu, D.-G. Huang, B.-T. Ann, and G.-C. Chang, "Applying fuzzy logic to control cycling movement induced by functional electrical stimulation," *IEEE Trans. Neural Syst. Rehabil. Eng.*, vol. 5, no. 2, pp. 158–169, Jun. 1997.

[16] Y. Ogawa, T. Inoue, T. Inada, Y. Tagawa, K. Yoshimitsu, and N. Shiba, "Locomotion assistance for the person with mobility impairment: Fuzzy control of cycling movement by means of surface electrical-stimulation," in *Proc. 29th Int. Conf. IEEE EMBS*, Aug. 2007, pp. 2420–2423.

[17] C.-S. Kim, G.-M. Eom, K. Hase, G. Khang, G.-R. Tack, J.-H. Yi, and J.-H. Jun, "Stimulation pattern-free control of FES cycling: Simulation study," *IEEE Trans. Syst. Man Cybern. Part C Appl. Rev.*, vol. 38, no. 1, pp. 125–134, Jan. 2008.

[18] P.-F. Li, Z.-G. Hou, F. Zhang, M. Tan, H.-B. Wang, Y. Hong, and J.-W. Zhang, "An FES cycling control system based on CPG," in *Proc. 31st Ann. Int. Conf. IEEE EMBS*, 2009, pp. 1569–1572.

[19] A. Farhoud and A. Erfanian, "Fully automatic control of paraplegic FES pedaling using higher-order sliding mode and fuzzy logic control," *IEEE Trans. Neural Syst. Rehabil. Eng.*, vol. 22, no. 3, pp. 533–542, 2014.

[20] T. E. Johnston, "Biomechanical considerations for cycling interventions in rehabilitation," *Phys. Ther.*, vol. 87, pp. 1243–1252, 2007.

[21] K. J. Hunt, C. Ferrario, S. Grant, B. Stone, A. N. McLean, M. H. Fraser, and D. B. Allan, "Comparison of stimulation patterns for FES-cycling using measures of oxygen cost and stimulation cost," *Med. Eng. Phys.*, vol. 28, no. 7, pp. 710–718, Sep. 2006.

[22] M. Gföhler and P. Lugner, "Dynamic simulation of FES-cycling: Influence of individual parameters," *IEEE Trans. Neural Syst. Rehabil. Eng.*, vol. 12, no. 4, pp. 398–405, Dec. 2004.

[23] E. S. Idsø, T. Johansen, and K. J. Hunt, "Finding the metabolically optimal stimulation pattern for FES-cycling," in *Proc. Conf. Int. Funct. Electrical Stimulation Soc.*, Bournemouth, U.K., Sep. 2004.

[24] N. A. Hakansson and M. L. Hull, "Can the efficacy of electrically stimulated pedaling using a commercially available ergometer be improved by minimizing the muscle stress-time integral?," *Muscle Nerve*, vol. 45, no. 3, pp. 393–402, Mar. 2012.

[25] L. A. Bremner, K. E. Sloan, R. E. Day, E. R. Scull, and T. Ackland, "A clinical exercise system for paraplegics using functional electrical stimulation," *Paraplegia*, vol. 30, pp. 647–655, 1992.

[26] D. Liberzon, *Switching in Systems and Control*. Boston, MA, USA: Birkhauser, 2003.

[27] N. Sharma, K. Stegath, C. M. Gregory, and W. E. Dixon, "Nonlinear neuromuscular electrical stimulation tracking control of a human limb," *IEEE Trans. Neural Syst. Rehabil. Eng.*, vol. 17, no. 6, pp. 576–584, Jun. 2009.

[28] M. J. Bellman, T.-H. Cheng, R. Downey, and W. E. Dixon, "Cadence control of stationary cycling induced by switched functional electrical stimulation control," in *Proc. IEEE Conf. Decis. Control*, 2014.

[29] J. L. Alberts, S. M. Linder, A. L. Penko, M. J. Lowe, and M. Phillips, "It is not about the bike, it is about the pedaling: Forced exercise and Parkinson's disease," *Exerc. Sport Sci. Rev.*, vol. 39, no. 4, pp. 177–186, Jun. 2011.

[30] G. M. Earhart and M. J. Falvo, "Parkinson disease and exercise," *Compr. Physiol.*, vol. 3, pp. 833–848, Apr. 2013.

[31] E. S. Idsø, "Development of a mathematical model of a rider-tricycle system," Tech. Rep. NTNU, Dept. Engineering Cybernetics, 2002.

[32] M. Gföhler and P. Lugner, "Cycling by means of functional electrical stimulation," *IEEE Trans. Rehabil. Eng.*, vol. 8, no. 2, pp. 233–243, Jun. 2000.

[33] J. L. Krevolin, M. G. Pandy, and J. C. Pearce, "Moment arm of the patellar tendon in the human knee," *J. Biomech.*, vol. 37, no. 5, pp. 785–788, 2004.

[34] D. A. Winter, *Biomechanics and Motor Control of Human Movement*. New York, NY, USA: Wiley, 1990.
[35] O. M. Rutherford and D. A. Jones, “Measurement of fibre pennation using ultrasound in the human quadriceps in vivo,” *Eur. J. Appl. Physiol. Occup. Physiol.*, vol. 65, pp. 433–437, 1992.
[36] M. Ferrarin and A. Pedotti, “The relationship between electrical stimulus and joint torque: A dynamic model,” *IEEE Trans. Rehabil. Eng.*, vol. 8, no. 3, pp. 342–352, Sep. 2000.
[37] T. Schauer, N. O. Negård, F. Previdi, K. J. Hunt, M. H. Fraser, E. Ferchland, and J. Raisch, “Online identification and nonlinear control of the electrically stimulated quadriceps muscle,” *Control Eng. Pract.*, vol. 13, no. 9, pp. 1207–1219, Sep. 2005.
[38] C. Cai, A. Teel, and R. Goebel, “Smooth Lyapunov functions for hybrid systems Part II: (Pre)asymptotically stable compact sets,” *IEEE Trans. Automat. Contr.*, vol. 53, no. 3, pp. 734–748, Mar. 2008.
[39] M. M. Hoehn and M. D. Yahr, “Parkinsonism: Onset, progression and mortality,” *Neurol.*, vol. 17, no. 5, pp. 427–442, 1967.
[40] J. Szecsi, P. Krause, S. Krafczyk, T. Brandt, and A. Straube, “Functional output improvement in FES cycling by means of forced smooth pedaling,” *Med. Sci. Sports Exerc.*, vol. 39, no. 5, pp. 764–780, May 2007.
[41] P. C. Eser, N. Donaldson, H. Knecht, and E. Stussi, “Influence of different stimulation frequencies on power output and fatigue during FES-cycling in recently injured SCI people,” *IEEE Trans. Neural Syst. Rehabil. Eng.*, vol. 11, no. 3, pp. 236–240, Sep. 2003.

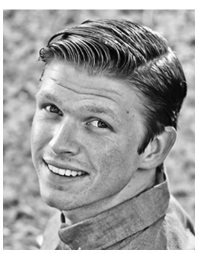

Matthew J. Bellman received the bachelor’s and master’s degrees, *magna cum laude*, in mechanical engineering with a minor in biomechanics from the University of Florida, Gainesville, FL, USA. He is currently pursuing the Ph.D. degree in mechanical engineering as a National Defense Science and Engineering (NDSEG) Fellow, with a continued focus on the theoretical development of robust, adaptive control systems for applications involving functional electrical stimulation, specifically those involving rehabilitation and mobility of the lower extremities.

He has been a member of the Nonlinear Controls and Robotics group, University of Florida, since May 2009.

Mr. Bellman’s work has been recognized by the American Automatic Control Council (AACC) O. Hugo Schuck (Best Paper) Award, in 2009 and 2015.

Teng-Hu Cheng received the B.Sc. and M.Sc. degrees in mechanical engineering from National Taiwan University, Taiwan, in 2007 and 2009, respectively. He is currently with the Nonlinear Controls and Robotics lab, University of Florida, Gainesville, FL, USA pursuing the Ph.D. degree under the supervision of Dr. Warren Dixon.

During the summers of 2013 and 2014, he was a Research Intern with Air Force Research Laboratory (AFRL) at Eglin AFB and University of Florida REEF, aiding in designing cooperative control for networked systems with time-varying network topologies and developing event-driven control for networked systems. His research interests include networked system control, switched control, event-driven control, and nonlinear control.

Ryan J. Downey received the B.S. degree in mechanical engineering from the University of Florida, Gainesville, FL, USA, in 2010, where he participated in a research experiences for undergraduates program (REU). He subsequently joined the Nonlinear Controls and Robotics group in 2010 to pursue his doctoral research. In 2011, he was accepted to an international exchange program (Atlantis CRISP) and received the M.S. degree in biomedical engineering from Politecnico di Milano, in 2012. Upon returning to the U.S., he received the M.S. degree in biomedical engineering from the University of Florida, in 2012, as well as the M.S. and Ph.D. degrees in mechanical engineering in 2014 and 2015, respectively.

He is currently a Postdoctoral Scholar at the Medical University of South Carolina. His research focuses on functional electrical stimulation, Lyapunov-based nonlinear control, and rehabilitation following stroke and spinal cord injury.

Dr. Downey’s work has been recognized by the 2015 American Automatic Control Council (AACC) O. Hugo Schuck Best Paper Award.

Chris J. Hass is an Associate Professor in the Department of Applied Physiology and Kinesiology, University of Florida, Gainesville, FL, USA. Prior to returning to UF, he held academic positions at Columbia University and Georgia Institute of Technology. Currently, he conducts research and teaches in the areas of biomechanics and motor control. He is an executive board member of the Biomechanics Interest Group within the American College of Sports Medicine and serves as an external reviewer for numerous scientific journals. He has received several teaching and research awards.

Warren E. Dixon received the Ph.D. degree in 2000 from the Department of Electrical and Computer Engineering, Clemson University, Clemson, SC, USA.

He was selected as an Eugene P. Wigner Fellow at Oak Ridge National Laboratory (ORNL). In 2004, he joined the Mechanical and Aerospace Engineering Department, University of Florida, Gainesville, FL, USA. His main research interest has been the development and application of Lyapunov-based control techniques for uncertain nonlinear systems. He has published three books, an edited collection, 12 chapters, and over 100 journal and 200 conference papers.

Dr. Dixon’s work has been recognized by the American Automatic Control Council (AACC) O. Hugo Schuck (Best Paper) Award, in 2009 and 2015, the 2013 Fred Ellersick Award for Best Overall MILCOM Paper, a 2012 and 2013 University of Florida College of Engineering Doctoral Dissertation Mentoring Award, the 2011 American Society of Mechanical Engineers (ASME) Dynamics Systems and Control Division Outstanding Young Investigator Award, the 2006 IEEE Robotics and Automation Society (RAS) Early Academic Career Award, an NSF CAREER Award (2006 to 2011), the 2004 Department of Energy Outstanding Mentor Award, and the 2001 ORNL Early Career Award for Engineering Achievement. He is an IEEE Control Systems Society (CSS) Distinguished Lecturer. He currently serves as a member of the U.S. Air Force Science Advisory Board and as the Director of Operations for the Executive Committee of the IEEE CSS Board of Governors.